FINAL

Send Orders for Reprints to reprints@benthamscience.ae

Current Protein and Peptide Science, 2016, *17*, 000-000

Pentameric Models as Alternative Molecular Targets for the Design of New Antiaggregant Agents

Exequiel E. Barrera Guisasola[a,b], Lucas J. Gutierrez[a,c], Sebastián A. Andujar[a,b], Emilio Angelina[b,c], Ana M. Rodríguez[a,b] and Ricardo D. Enriz[a,b,*]

[a]*Facultad de Química Bioquímica y Farmacia, Universidad Nacional de San Luis, Chacabuco 915, 5700 San Luis, Argentina.* [b]*IMIBIO-SL (CONICET), Chacabuco 915, 5700 San Luis, Argentina.* [c]*Laboratorio de Estructura Molecular y Propiedades, Área de Química Física, Departamento de Química, Facultad de Ciencias Exactas y Naturales y Agrimensura, Universidad Nacional del Nordeste, Avda. Libertad 5460, 3400 Corrientes, Argentina*

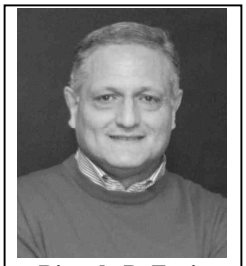

Ricardo D. Enriz

Abstract: The structure-based drug design has been an extremely useful technique used for searching and developing of new therapeutic agents in various biological systems. In the case of AD, this approach has been difficult to implement. Among other several causes, the main problem might be the lack of a specific stable and reliable molecular target. In this paper the results obtained using a pentameric amyloid beta (Aβ) model as a molecular target are discussed. Our MD simulations have shown that this system is relatively structured and stable, displaying a lightly conformational flexibility during 2.0 μs of simulation time. This study allowed us to distinguish characteristic structural features in specific regions of the pentamer which should be taken into account when choosing this model as a molecular target. This represents a clear advantage compared to the monomer or dimer models which are highly flexible structures with large numbers of possible conformers. Using this pentameric model we performed two types of studies usually carried out on a molecular target: a virtual screening and the design on structural basis of new mimetic peptides with antiaggregant properties. Our results indicate that this pentameric model might be a good molecular target for these particular studies of molecular modeling. Details about the predictive power of our virtual screening as well as about the molecular interactions that stabilize the mimetic peptide-pentamer Aβ complexes are discussed in this paper

Keywords: Pentameric model, molecular target, MD simulations, antiaggregant compounds, virtual screening, mimetic peptides.

1. INTRODUCTION

Amyloid fibril formation is associated with a wide number of incurable diseases [1]. The increasing incidence of neurodegenerative disorders could be partially attributed to the substantial increase in the mean lifespan in developed countries, and to a growing list of such disorders including Alzheimer's, Parkinson's, Huntington's and the prion diseases all of which are associated with the aggregation of proteins into amyloid fibrils. These disorders, also known as amyloidosis, are characterized by the misfolding and aggregation of specific proteins that accumulate intracellularly or extracellularly in the brain as insoluble deposits and interfere with the biological functions [2, 3]. Alzheimer's disease (AD) is the most common cause of dementia among neurodegenerative disorders in the elderly population, affecting about 25 million people worldwide. It has been estimated that the number of affected people will double every 20 years [4]. While there is significant research ongoing to find therapeutics to combat amyloid diseases, it is important to first understand and appreciate the various structural and physicochemical properties of amyloid fibrils in order to design better therapeutics for treating this class of diseases.

It is important to note that while drug design based on structure has been extremely useful for searching and developing of new therapeutic agents in various biological systems, this approach has been very problematic and difficult to implement in the particular case of AD.

Limitations of a Structure-Based Design in the Case of AD

The structure-based drug discovery is a very well-known strategy that has been effective in identifying small-molecule ligands that bind to the native states of globular proteins [5, 6]. In this way, our research group has already reported several studies by using this strategy [7-10]. It should be noted that this type of rational approach requires of previous information and is subjected to several factors:

i. physiological evidence to understand the disease or problem in such a way that allows us to hypothesize that a drug with a particular action could be beneficial from a therapeutic point of view.

*Address correspondence to this author at the Facultad de Química Bioquímica y Farmacia, Universidad Nacional de San Luis, Chacabuco 915, 5700 San Luis, Argentina. IMIBIO-SL (CONICET), Chacabuco 915, 5700 San Luis, Argentina; Tel: (54) 2652.423789; E-mail: denriz@unsl.edu.ar

1389-2037/16 $58.00+.00

ii. a molecular target (structural information about the active site)

iii. an explicit starting point (from the chemical point of view).

iv. bioassays to evaluate the activity of potential ligands so that they can be related to the potential therapeutic effect.

Unfortunately, several of these requirements are at least questionable in the case of the design on structural basis of new antiaggregant agents.

Regarding the first item (i) it is well documented that AD is a disease with multifactorial causes and therefore there are different hypotheses that might explain the reasons for this disease [11, 12]. Probably the Aβ hypothesis is one of the most accepted; it has been questioned and is currently under discussion [13, 14].

Taking as valid the Aβ hypothesis, a possible molecular target arising is the inhibition of β-secretase (BACE1). Besides a catalytic site, this enzyme has an exosite, our group being the first to predict its exact location by means of a blind docking study [15]. Later, our results were experimentally corroborated by two simultaneous studies using antibodies [16, 17], thus demonstrating the great utility of the blind docking techniques [15]. While there are numerous reports of compounds with inhibitory properties on the catalytic site of BACE1, unfortunately none of them is a therapeutic option. Among others, the pharmacokinetic aspects constitute a serious problem for the development of new drugs with this property [18, 19].

On the other hand it should be noted that trying to find a reliable molecular target for the design of new antiaggregant agents using oligomers as a structural base is a particularly complicated and difficult situation. A particular difficulty in this issue is the deficit of a specific and stable structure of the molecular target [20] that would allow efficient screening of potential pharmacophores *in silico* or *in vitro* (item (ii)). The absence of well-defined structures is by far the main cause of the current reality in which neither the protein self-assembly process nor the molecular interactions of the small molecules with their target are sufficiently understood [21]. Due to these obstacles, most efforts geared at discovering and testing new protein oligomerization inhibitors/ modulators for different amyloid-related diseases have relied on empirical observations [22]. The inherent problem to the item iii) is largely related to the lack of a single molecular target. Nevertheless, in the last decade many studies have been made in the search of new antiaggregant compounds. Although numerous compounds have been reported with this property, progress in this area is very slow and it has not yet managed the finding of a compound that might be successfully used for therapeutic purposes. There are several reasons for this situation. First, the type of molecules and how most of these compounds have been obtained have to be considered. Predominantly, there are two types of compounds: peptides derived from the Aβ protein sequence [23, 24], or obtained through *in vitro* or *in silico* screening [25-27], and small molecules obtained empirically [28, 29]. A very confusing aspect with these compounds is that their mechanisms of action are poorly understood even at the level of *in vitro* experiments. As a result, studies involving more complex cellular and whole-animal systems often lead to further complication and discrepancy, and correlating studies using different systems or performed by different research groups might be somewhat erratic (problems related with item iv). Many compounds influence the aggregation pathway of amyloidogenic proteins in distinct ways. Interestingly, compounds as diverse as polyphenols, sugar derivatives, peptides, and artificial receptors, such as molecular tweezers, bind directly to different amyloidogenic proteins and often yield similar effects on the aggregation pathways, whereas in other cases, compounds with similar structures exert opposite effects, such as inhibition or acceleration of fibril formation.

Finally, it must be pointed out that there are two major challenges in the use of this approach into intrinsically disordered proteins. The first one, is the existence of very substantial technical difficulties in acquiring accurate information about the structure and dynamics of disordered proteins by experimental methods (problems related to item iv) [30-32]; and the second one is that the binding pockets in these molecules are likely to be present only transiently.

The road to this goal is undoubtedly very arduous as many different factors play a significant role in the design of new drugs on structural basis. A possible solution might be to dissect the problem into simple steps, which are open to the available tools and permit us at least partial answers. One major step is the study of potential molecular targets, which are necessary to develop new approaches to decipher the molecular interactions and mechanisms by which inhibitors and modulators of aggregation exert their effects. This will be crucial in the generation of new agents with potential therapeutic use for diseases caused by aberrant protein folding and aggregation.

Why a Pentameric Model as a Potential Molecular Target?

Following the initial association of two monomers into a dimer in the early steps of the formation of amyloid fibrils, the assemblies are classified loosely as oligomers, an imprecise definition describing a variety of species that are water-soluble, metastable, and inevitably exist as mixtures of multiple structures which in most cases are cytotoxic [33, 34]. Thus, within the broad definition of oligomers, there are different forms, which might be considered as potential candidates to be used as molecular targets.

Although the Aβ monomer has been used as a molecular target [35, 36], this structure has very particular structural features that make it a very poor candidate to fulfill this role. This peptide is highly disordered in solution, populating a heterogeneous ensemble of conformations [37, 38]. Unfortunately, experimental studies aimed at the detailed characterization of monomeric structures (e.g. crystallization) at physiological conditions have been greatly hindered by the high aggregation rates of the Aβ peptides, as well as their sensitivity to specific physicochemical conditions. Nevertheless, distinctive features of the monomers in water have been elucidated using NMR techniques. Further insights into the Aβ monomer structures and their aggregation mechanism have been derived from diverse computational approaches using explicit or implicit solvent [39, 40]. However, notably

dissimilar results for analogous systems are found in many of these studies; such inconsistencies might be mainly attributed to the specific sequence and length of the modeled segments, as well as to the effect of the force field and solvation model on the dynamics of this flexible peptide. Although most of these studies may correctly describe some monomer features, like total β-sheet/helical content, a full validation of an appropriate *in silico* model for Aβs and their aggregates at physiological conditions might entail comparison with yet-unknown experimental structures. In short, despite numerous experimental and computational efforts, there is still not a clear picture of the key structural features of the monomers that may seed the oligomerization process.

The conformational intricacies of the Aβ monomer are huge. Therefore, to correctly analyze its conformational behavior, techniques such as replica exchange or metadynamics, which are approaches highly demanding of computing time, are necessary. Considering that on a molecular target numerous simulations for a large set of compounds might be performed, it is evident that the monomer model is not a good candidate to be used as a molecular target, at least not to perform systematic studies using the usual techniques.

The dimer situation is not very different from that of the monomer. Although the dimer is somewhat less flexible than the monomer, long simulations are also required using replica exchange and metadynamics in order to perform the conformational study of the dimer appropriately. The studies reported by Derremaux *et al.*, among others, illustrate this situation very well [41, 42].

The conditions of the monomer and dimer are in sharp contrast to that of the fibrillar state of the peptide, which is very ordered and has been characterized in general terms, notably by X-ray fiber diffraction [43], electron microscopy and solid-state NMR studies [44]. An intermediate situation can be found in structures such as the pentamer. This type of structure is soluble but still, well structured and much more stable than the monomer or dimer. Such structural characteristics clearly make the pentamer a better candidate as a molecular target, at least to perform exploratory studies of potential new antiaggregant compounds.

In this paper, we have tested a pentameric model as a molecular target for the search of new antiaggregant agents. This model has been used for the realization of a virtual screening as well as for studies of molecular dynamics simulations of mimetic peptides acting as new antiaggregant agents. The advantages and disadvantages of using this type of pentameric model will be discussed throughout this work.

2. RESULTS AND DISCUSSION

Once we have decided to study the pentamer as a potential molecular target, the next step was to select a pentameric model to test it. The structure of $A\beta_{1-42}$ was obtained from the Protein Data Bank (PDB code, 2BEG). This model lacks the first 16 residues. Therefore, in order to have the full molecule of $A\beta_{1-42}$, the sequence for the residues 1-17 was completed using a random coil segment. In this model, each Aβ monomer in the fibril presents a highly flexible disordered region (DR) (residues 1-17) and a β-strand–turn–β-strand motif (residues 18-42) that contains two intermolecular, parallel, in-register β-sheets that are formed by residues 18–26 (β1) and 31–42 (β2).

Structural Changes Observed for the Pentameric Model During 2 μs of Simulation

In the first stage of our study, we performed MD simulations (with a total time of 2 μs) to evaluate the structural changes that might occur during the simulation time. In order to determine the more significant structural features, it was necessary to make a quantitative study using different parameters or molecular descriptors.

The root mean square deviation (rmsd) of backbone atoms was calculated to measure the flexibility of the model. The analysis was divided into two different regions, β1 and β2, in order to present the results more clearly. The rmsd analysis of DR was not included due to its inherent great flexibility. In general terms, a significant stability can be observed during the simulation time, displayed by plateau regions seen in most of the graphics (Fig. **S1**, supporting information). In addition we also observed situations in which the rmsd values fluctuate above normal values, e.g. the increase of flexibility in β1 region that can be partially explained by the augmenting distances between adjacent chains leading to the formation of interchain cavities as result of the loss of its stabilizing hydrogen bonds (Fig. **1**). Also, in the case of β2 region different typical conformations reflected by the variations in the rmsd values (Fig. **S2**) were observed, such as a tightly organized β-helix formation (Fig. **2**).

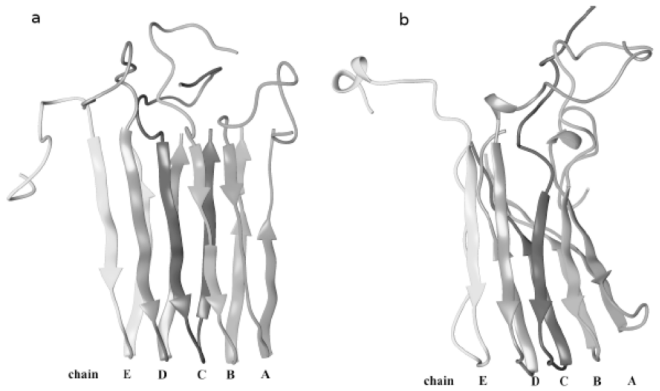

Fig. (1). Snapshots of the $A\beta_{1-42}$ pentamer comparing: **a**) the initial structure and **b**) the final conformation obtained from one of the ten MD simulations. Here, we can see the partial dissociation between adjacent chains in the β1 region.

Continuing the structural analysis, interchain distances were measured showing differentiated behaviors for each region. It should be noted that the packing between monomers was higher in β2 region. For this region, distances between alpha carbons of residues Ile32, Leu34 and Val36 of adjacent chains were selected. As for β1 region, the residues selected were Phe19 and Glu22; in this case the distances were bigger than those observed for β2 (Fig. **S3**, supporting information). These results are in agreement with the above mentioned cavities. It should be noted that this spatial ordering was also observed in a pentameric model previously reported by our group [45]. Such model was successfully used in the design of new mimetic peptides with antiaggregant

properties [46]. Another critical portion of the Aβ is the so called TOP site, where an incoming monomer may take position during the oligomerization process. This is an interesting area in two different ways: on one hand, this zone could be "capped" by small ligands occupying the backbone hydrogen bonding groups of the peptides. On the other hand an increase of the distance between β1 and β2 regions might allow the entry of potential ligands favoring their interaction with the hydrophobic core of the pentamer (Fig. **3**). This type of interactions has been previously reported by our group in the study of Amyloid-β fibril disruption by fullerene [47]. This distance was measured using the alpha carbons of the following pairs of confronted residues: Glu22-Leu34, Asp23-Gly33 and Val24-Ile32 (Fig. **S4**, supporting information).

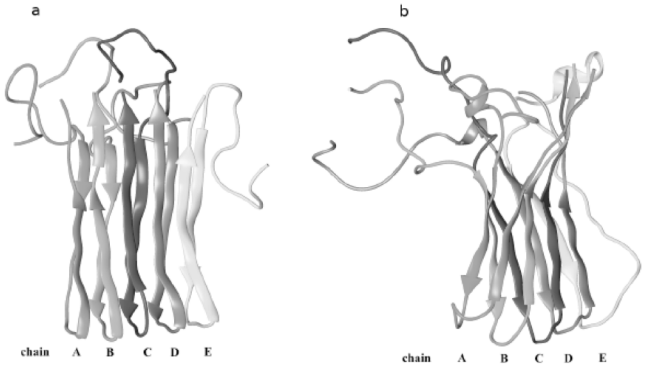

Fig. (2). Snapshots of the $A\beta_{1-42}$ pentamer comparing: **a**) the initial structure, and **b**) the final conformation obtained from one of the ten MD simulations. Here, we can see the tightly organized β-helix formation located in the β2 region.

Our 2 μs molecular simulations revealed that the β-strand twist was a distinctive element of the pentamer, with a compact packing of side chains forming a laminated "steric zipper" interface between the β-sheets. Furthermore, our MD simulations suggested that during the simulation time, although the aforementioned motif is maintained, certain openings between adjacent chains are formed, particularly in the β1 portion. This situation should be taken into account when selecting a pentameric model as a molecular target, as it includes new potential binding sites that may not be feasible to consider by using the highly compact structure, reported in the PDB.

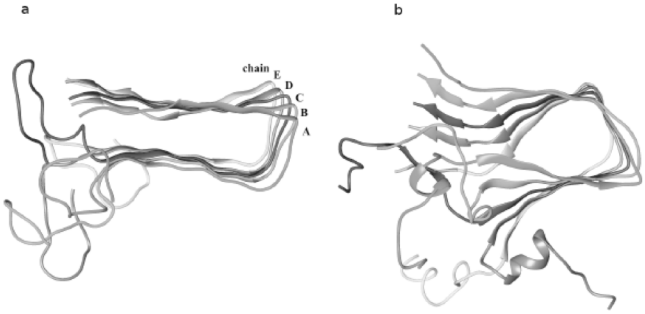

Fig. (3). Snapshots of the $A\beta_{1-42}$ pentamer comparing: **a**) the initial structure, and **b**) the final conformation obtained from one of the ten MD simulations. Here, we can see the increased distance between β1 and β2 portions in the so called TOP region.

In order to confirm the stability of this model we extend to 600 ns the simulations for two replicas, taking as starting structure their respective final points obtained from the 200 ns MD simulations. As we expected, the structures remain compact in the beta regions, showing only the characteristic distortion in the disordered region (Fig. **S5**, supporting information).

After the conformational behavior of the pentameric model was studied by long simulations, this model was validated with two types of studies usually performed on a molecular target: i) a virtual screening and ii) the design on structural basis of new mimetic peptides with antiaggregant properties.

Virtual Screening using a Pentameric Model

In this study, the virtual screening of known inhibitors of Aβ aggregation was performed using a structure of a pentamer formed by full Aβ peptides ($A\beta_{1-42}$) as a model for amyloid protofibril. The principal aim of this study is to evaluate if the pentameric model is a molecular target useful for this study. An additional goal is to provide more clues about where these known inhibitors might bind to amyloid fibril and how they might inhibit further fibril elongation. This information might be useful for rational drug design of novel inhibitors targeting fibril formation in Alzheimer's disease.

Due to the lack of atomic-level information about how small molecules bind to amyloid fibrils composed of full $A\beta_{1-42}$ units, the entire Aβ pentamer surface was explored by performing a blind rigid docking of the ligand dataset with the AutoDock Vina program in order to find putative binding sites [48].

Fig. **4** shows the docking poses obtained from the blind rigid docking analysis. Most of the molecules bind at one pentamer end, either in the disordered region or in a cleft formed by strands β1 and β2. Interestingly, this is the same end (termed the odd end) suggested before as the growing end of the protofibril [49]. As discussed elsewhere, intermolecular side-chain contacts are formed between the odd-numbered residues of strand β1 of the nth molecule and the even-numbered residues of strand β2 of the $(n - 1)$th molecule. This interaction pattern implies the presence of distinct surfaces at the opposing ends, which explains the sequence selectivity, the cooperativity, and the apparent unidirectionality of Aβ fibril growth [49].

Recent studies have pointed out that binding of inhibitors to the edge of amyloid fibrils can block the attachment of the incoming peptide, suggesting that this binding site can serve as a potential inhibition site to stop β-strand elongation [50].

In addition to the blind docking screen, we have also explored the entire pentamer surface with the AutoLigand (AL), a grid-based method to predict ligand-binding sites in proteins of known structure [51]. In short, the user first calculates an affinity potential grid around the protein, and then a flood-fill and a site-optimization process are used to identify the best contiguous envelopes within the energy grid. One of the advantages of AL with respect to other binding site prediction methods is that it uses a full atomic representation, with atom types for carbon, hydrogen, oxygen and

others (if desired), to yield a chemically detailed prediction of the shape of a ligand within a predicted binding site.

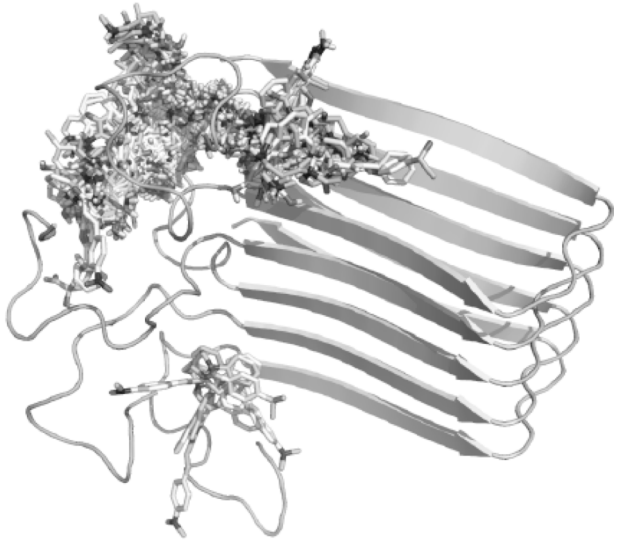

Fig. (4). Docking poses obtained from the blind rigid docking.

Fig. **5** shows the six best contiguous envelopes found by AL, excluding the envelopes for the disordered region (left view). The envelopes are numbered in decreasing order of magnitude of their energy per volume (EPV) ratio from greater (I) to lowest (VI) ratio. The greater the EPV ratio in magnitude, more favorable is the binding in that site. The envelopes obtained from AL suggest three putative binding sites. Site V (in light blue) located along the growing end/edge of the pentamer, which is in agreement with the results obtained from the blind rigid docking. Moreover, AL predicted two additional binding sites: one at the extended β2-sheet surface (site VI, in green) and another one at the laminated "steric zipper" interface between the β-sheets, where four distinct envelopes (I to IV) might be observed. It is not surprising that AL has found more binding sites than the blind rigid docking screen of the active/inactive dataset. Considering that an AL envelope is subjected to optimization cycles of its shape and types of atoms probes, it is possible to reach those sites on the rigid pentamer surface (in particular the steric zipper interface between the two β-sheets) which are not easily accessible for actual molecules with a definite structure.

Taking into account the previous results, we decided to perform a new docking experiment of the active/inactive dataset, but now adding some flexibility in the molecular target ($A\beta_{1-42}$ pentamer) to see if some molecules from the dataset are able to reach some of the binding sites in the steric zipper interface, as predicted by AL.

We hypothesize that the most effective fibril-growth inhibitors will be those that, while lying in the fibril edge as predicted by the blind rigid docking, also show some insertion into the steric zipper interface. Since the growing edge of the fibril (i.e. binding site V) would be exposed to the solvent, an extra-anchoring of the ligands in the hydrophobic, steric zipper interface might decrease their dissociation rate due to solvent exposure, thus increasing its binding affinity.

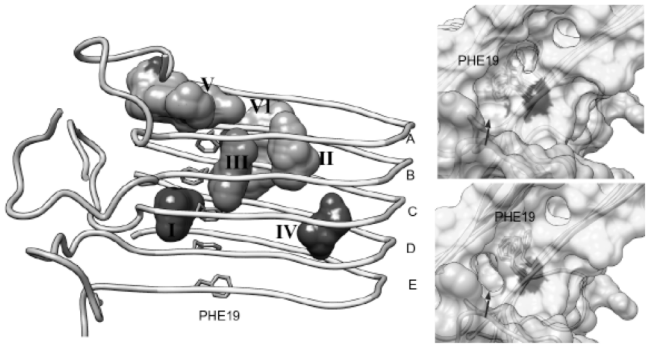

Fig. (5). The best contiguous envelopes found by AL, excluding the envelopes for the disordered region (left view). The envelopes are numbered in decreasing order of magnitude of their EPV ratio from greatest (I) to lowest (VI) ratio.

Fig. **5** (left view) shows that the side chain of Phe19 from $A\beta_{1-42}$ (monomers A and B) occluded a channel that connects site V on the growing end of the fibril with the site I in the steric zipper interface. Fig. **5** (right part) also shows how the displacement of the phenylalanine side chains opens/closes the channel connecting site V to the site I. As the phenylalanine side chains are allowed to freely rotate in solution, those phenylalanine residues are more flexible in the virtual screening experiments, and therefore we are constructing a more reliable (more flexible) model of the fibril that, in addition, might allow an extra-anchoring at site I.

On the basis of the previous results, we decided to perform a more site-focused, flexible docking screening for the balanced dataset of active/inactive compounds. Thus, the ligands were docked into the β-strand region of the fibril with the (automatically computed) potential grid maps encompassing not the entire protein but only sites I, II, III, V and VI. Most of the disordered fibril region was left out of the grid box since any structure joined here probably represents just a momentary mode, due to the inherent flexibility of this region.

The flexibility of the fibril was taken into account by docking the ligands against seven rigid pentameric structures (ensemble docking) representing different conformations of Phe19 side chain from $A\beta_{1-42}$ monomers A, B and C (Phe19A, Phe19B and Phe19C, respectively). These structures are considering both, open and closed states of the channel which connects site I with V.

As shown in Fig. **6**, the new setup in the last docking experiment changed notoriously the docking poses with respect to that obtained with the blind rigid docking. While some ligands just lie over the fibril-growing edge of the fibril model, other ligands have part of their structure buried into the channel previously identified in the steric zipper interface of the pentamer. Moreover, only one ligand, Congo Red, binds to the extended β2-sheet surface, termed as site VI in Fig. **5**.

Assessing the Performance of the Model

To assess the quality of our "flexible" fibril model as well as the overall performance of the protocol to predict the ligand binding sites, we used the Receiver Operating Charac-

teristic curves (ROC). ROC curves are produced by classifying data as positive or negative according to a threshold decision. The ROC curve is a plot of Sensitivity (Se) on the y-axis versus 1-Specificity (1-Sp) on the x-axis; calculated at intervals over the ordered list. This graphical technique is widely used in signal detection and medical statistics. In signal detection theory, Se is the perceived signal (in this case the activity) and 1-Sp is related to the detected background "noise" emitted by inactive molecules [52].

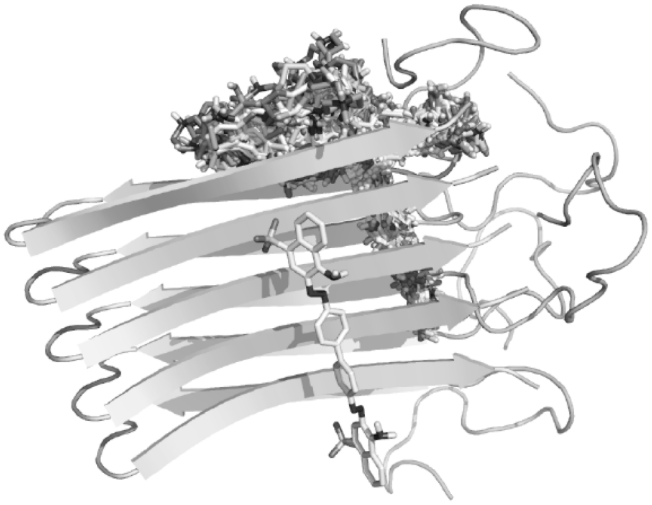

Fig. (6). The poses obtained from the site-focused, flexible docking. For each ligand, only the pose with the best docking scoring is depicted.

Fig. **7** shows the ROC curves obtained for the virtual screening of the database of active and inactive compounds as performed with Autodock Vina by using the flexible site-focused technique (black solid line) and the blind rigid technique (dashed line). In this graphic, the 45° diagonal (gray line) represents a random classification of the database with an area under the curve (AUC) for the random case of 0.5. Any model with an AUC > 0.5 performs better than random in discriminating active compounds from inactive ones. As observed in the figure, both models perform better than random, but it is clear that the site-focused flexible docking has achieved a much better classification of the dataset than the blind rigid docking.

Having demonstrated a better performance of the site-focused flexible virtual screening protocol, we focused on the analysis of the docking poses predicted by this flexible model in order to obtain a more definite structure-activity relationship from these data (Fig. **8**). In this scatter plot, ligands that lie over the growing edge of the fibril model, with no insertions into the steric zipper interface of the fibril model, are depicted with blue empty circles while those ligands that are either partially or totally buried into the steric zipper interface are depicted with red empty circles. Centroids (i.e. mean values) for the distribution of buried and not buried scatter points are depicted in red and blue solid circles, respectively. As indicated by the centroid plot coordinates, the non-buried ligands show in average worst docking scores and higher log (IC50) values in comparison to the buried ligands. Thus, our docking results agree with the experimental data indicating that buried compounds, on average, are more active than the non-buried ones. These results support, at least in part, our hypothesis that the most effective fibril-growth inhibitors might be those that show some kind of insertion into the steric zipper interface. Moreover, our results show that the Aβ pentameric model is a good molecular target to perform this type of virtual screening.

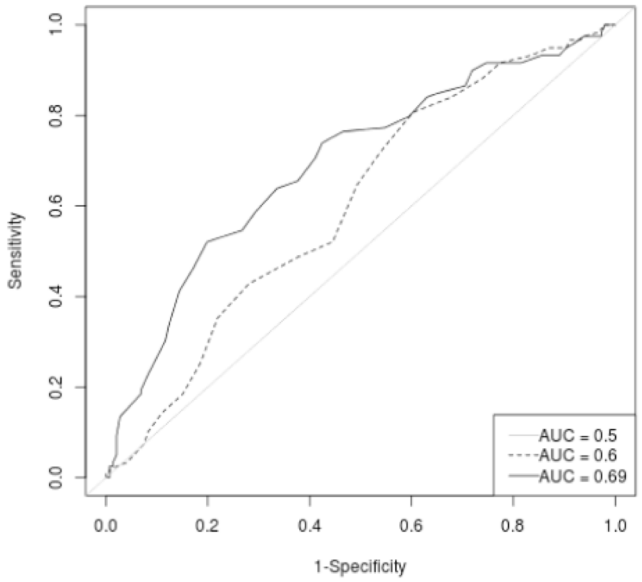

Fig. (7). The ROC curves obtained for the virtual screening of the database of active and inactive compounds.

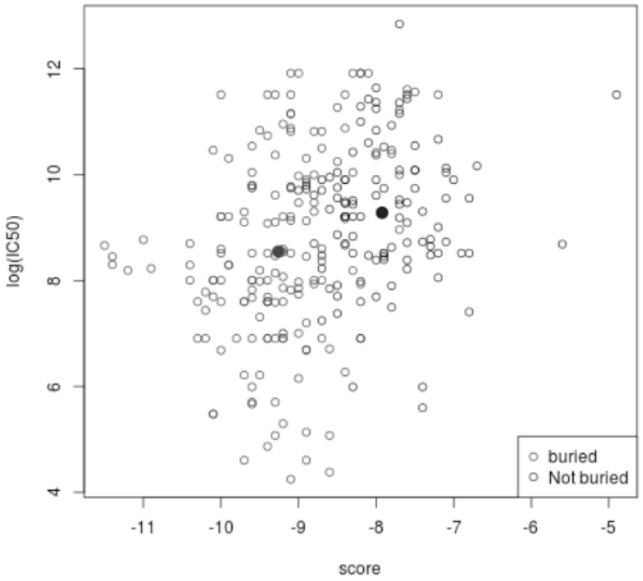

Fig. (8). A scatter plot of IC50 (in nM) logarithmic values *versus* the docking scoring (in kcal/mol) for the dataset of active/inactive compounds, as predicted by the site-focused flexible virtual screening.

Design of New Mimetic Peptides with Antiaggregant Effects by using a Aβ Pentameric Model

In a very recent paper, we reported two new mimetic peptides with antiaggregant properties. These compounds were designed from a molecular modeling by using a pentameric model as a molecular target [46]. Among the compounds tested, compound **2** displayed the strongest activity;

whereas compound **1** was taken as starting structure (Fig. **9 a** and **b**).

Interestingly, this model also allowed us to predict the lack of activity of other compounds used as negative controls in this series.

The synopsis of ThT assays, TEM studies and dot Blot assays allowed us to draw conclusions about the aggregate species formed by direct interactions between $A\beta_{1-42}$ and the above mentioned mimetic peptides. The content of well-ordered soluble fibrils was greatly diminished (ThT assays). The few remaining fibrillar components displayed a significantly altered morphology (TEM) and the dotblot results clearly indicated the inhibition of soluble toxic oligomers formation.

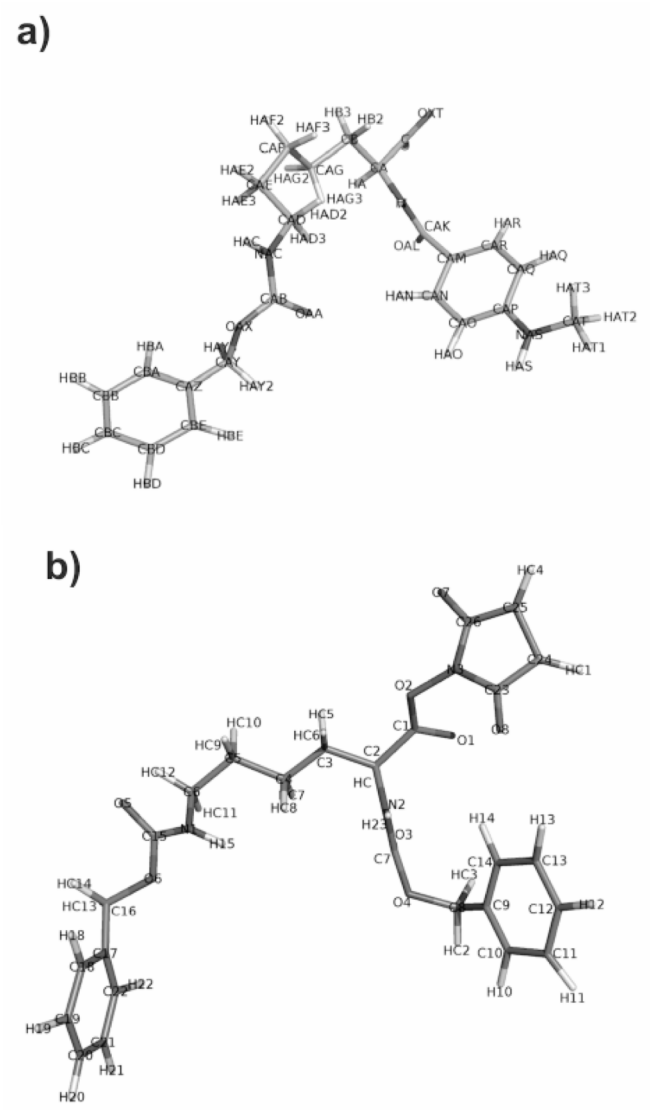

Fig. (9). Spatial views of **a**) compound **1** and **b**) compound **2**.

Our 200 ns MD simulations showed that these compounds act by binding β1 region, interacting with Phe19 and then internalizing in the central hydrophobic core. This produces the gradual opening of adjacent chains of the binding zone. It is important to remark that compounds **1** and **2** are deeply inserted into the hydrophobic core in contrast to the inactive compounds which are located in a more superficial way (Fig. **10**). An important aspect that was not studied in sufficient detail in our previous paper is the intermolecular interactions that occur between the different ligands in the binding site in the Aβ pentameric model. In order to complete this aspect, in this study we conducted a comprehensive analysis of molecular interactions of two different complexes by using a QTAIM study.

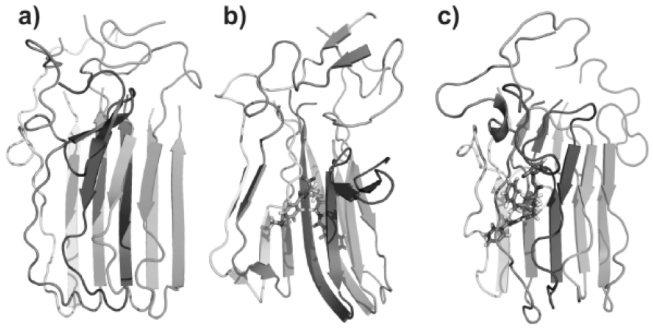

Fig. (10). Spatial view of **a**) pentamer, **b**) compound **2**– pentamer complex, and **c**) compound **1**–pentamer complex. The pentamer structure is shown in cartoon. The chains A, B, C, D and E are shown in yellow, orange, magenta, cyan and green, respectively. The inhibitors are shown in blue (compound **2**) and pink (compound **1**) sticks.

Analysis of the Binding Mode of Mimetic Peptide Compounds in the $A\beta_{1-42}$ Pentamer

In order to acquire a quantitative and more detailed insight into beta sheet breakers mechanism of compounds reported in reference 46, two representative mimetic peptides were evaluated. Thus, compound **1** (mimetic peptide taken as starting compound) and compound **2** (the strongest compound in the series) were selected for this study. The interactions between these compounds and the Aβ pentamer were analyzed by using QTAIM theory at the B3LYP-D/6-31G(d) level. Final snapshots of a 200ns MD simulation were used as input geometries in our QTAIM study.

Fig. **10** shows the structural conformation of the wild type (WT) pentamer, complex **1**-pentamer and complex **2**-pentamer (Figs. **10 a**, **b** and **c** respectively). The alteration of the packing of adjacent chains in the pentamer caused by the presence of inhibitors is clearly observed in this figure. Inhibitors are introduced into the β1 region between the B and C chains, causing the breaking of the inter-chain interactions which are responsible for the native structure of the pentamer.

Fig. **11a** shows the hydrophobic interactions present in the Aβ pentamer between Val36E and residues Phe19D (HG11Val36E•••HE2Phe19D,HG22Val36E•••HE2Phe19D), Phe19C(HG12Val36E•••HE1Phe19C,HG13Val36E•••HZPhe19C) and Ala21C (HG22Val36E•••HB3Ala21C, HG22Val36E•••HB2Ala21C); the nomenclature used for these atoms is shown in Fig. **9**. These interactions disappear in the presence of compounds **1** and **2** due to the strong interactions generated by a large number of hydrophobic contacts between Val36A and compounds **1** and **2** (Figs**. 11b** and **c**).

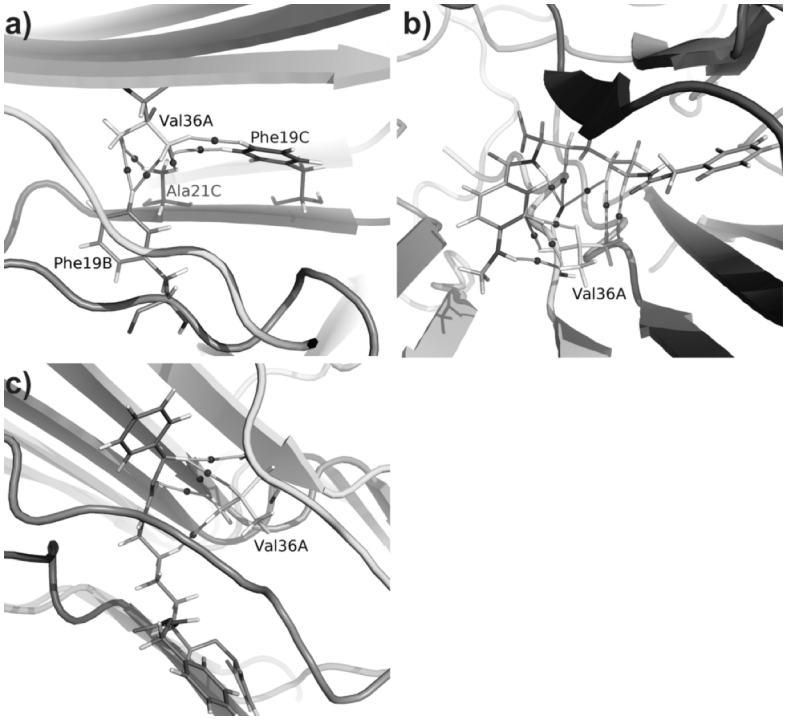

Fig. (11). Molecular graphs obtained for the non-covalent interactions for: **a**) the WT pentamer, **b**) compound **1**–pentamer complex, and c) compound **2**–pentamer complex; showing the elements of the electron density topology. The bond paths connecting the nucleus are represented in pink sticks and the bond critical points are shown as red spheres.

In the WT pentamer, Phe19B presents interactions with chain C through contacts CH•••π and CH•••H with Leu34B and Ala21C; whereas in the presence of compound **2** these interactions are mainly lost due to the formation of two hydrogen bonds between compound **2** and Phe19B (H23compound**2**•••OPhe19B,O2compound**2**•••HB2Phe19B) (Fig. **12 a** and **b**).

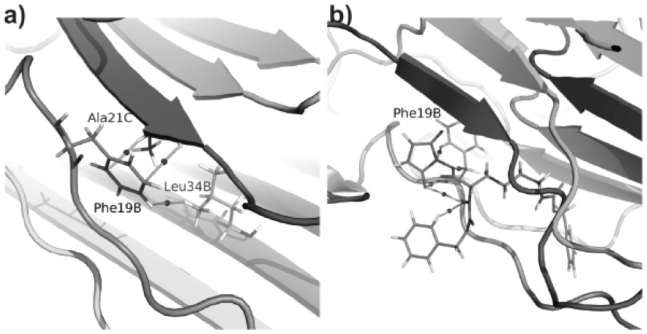

Fig. (12). a) Non-covalent interactions between Phe19C and Ala21C, Leu34D in the WT pentamer and **b**) non-covalent interactions between Phe19C and compound **1**.

In addition, compound **1** binds with great affinity to Lys16C by two strong hydrogen bonds (OXTcompound **1**•••HZ1Lys16C, OALcompound **1**•••HZ3Lys16C) (Fig. **13**). It should be noted that Lys16C, is located adjacent to the central hydrophobic cluster (residues 17-21), a key region in Aβ fibrillogenesis; hence, the bind of **1** in this region might alter the Aβ folding and therefore, produce a reduction in the amyloid aggregation [53].

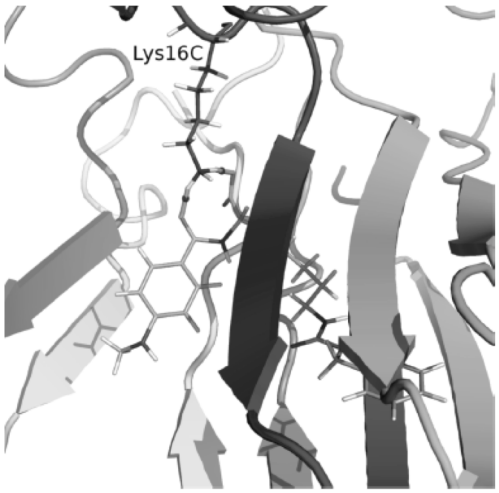

Fig. (13). Non-covalent interactions between Lys16C and compound **2**.

Another important residue of the Aβ pentamer is Phe19C. This amino acid contributes strongly to the binding between chains A, C and D through interactions of type CH•••π y CH•••H with Val36A, Gly38A, Ala21C and Phe19D. These interactions play a key role stabilizing the pentameric structure throughout the steric zipper interface between β1 and β2 regions. It should be noted that Phe19C is part of a central hydrophobic cluster (residues 17-21), and this sector is a key region in Aβ fibrillogenesis, as previously discussed. As seen in Fig. **14**, these specific interactions between the two β regions do not exist as result of the contacts between compounds **1** and **2** with Phe19C. Compound **1**

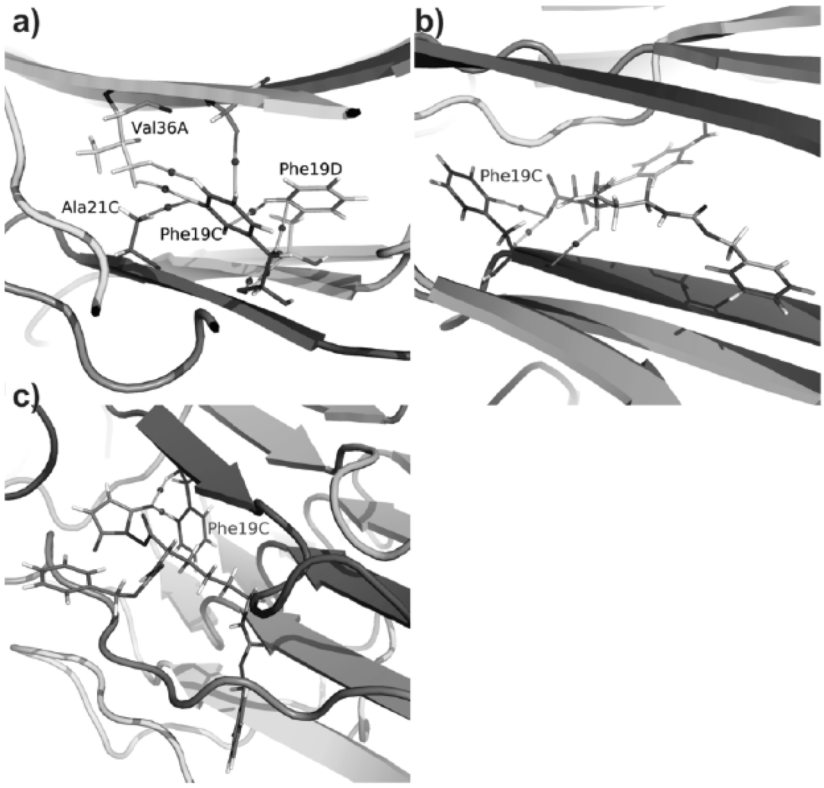

Fig. (14). Molecular graphs showing the non-covalent interactions for: **a**) the residue Phe19C in the WT pentamer, **b**) compound **1**–pentamer complex, and **c**) compound **2**– pentamer complex.

forms four hydrogen bonds whereas compound **2** presents two hydrogen bonds with Phe19C.

In summary, both compounds studied here join the central hydrophobic cluster, a key region in Aβ fibrillogenesis, that contains critical elements for Aβ self-assembly, as was experimentally demonstrated by the blocking of aggregation induced by mutating Val18, Phe19, and Phe20 [54]. The compounds discussed here present a high affinity with this region and adjacent residues, which might explain, at least in part, the higher activity as Aβ inhibitors. These results are consistent with those obtained in our virtual screening indicating that the most active compounds are those which are deeper inserted into the interface of the steric zipper interface.

3. METHODS

Molecular Dynamics Simulations

The geometry of the pentamer was soaked in boxes of explicit water using the TIP3P model [55] and then subjected to MD simulation. All MD simulations were performed with the Amber software package [56] using periodic boundary conditions and cubic simulation cells. The particle mesh Ewald method (PME) [57, 58] was applied using a grid spacing of 1.2 Å, a spline interpolation order of 4 and a real space direct sum cutoff of 10 Å . The SHAKE algorithm was applied [59] allowing for an integration time step of 2 fs.

Finally, the production was carried out at the NVT ensemble running 10 independent simulations with length limited to 200ns, accounting for a total simulation length of 2μs. Each individual simulation was started reading the final coordinates obtained from the equilibration phase but generating random initial velocities at the target temperature (irest = 0, tempi = 300K) and assigning different random seeds (ig = -1). Post MD analysis was carried out with program PTRAJ [56].

Dataset Compilation

As well as a model is designed to search for active molecules in a database, a validation method is designed to demonstrate the performance on this database which includes the pharmacological activity of these compounds. Screenings of such databases allow the validation of the model by assessing its ability to retrieve active molecules (true positives) and to discard the inactive ones [52].

Two extremes of the tests are generally applied in the literature, either seeding a few active compounds in a database of drug-like decoy molecules or using a highly focused set of active and inactive molecules [60]. In this last case, actually all compounds will show some activity; and therefore it is necessary to set a cutoff (i.e. Ki or IC50 values) above which compounds are considered as inactive. This second approach might be more accurate in discriminating what are the structural features that explain the different activity between active and inactive compounds. Therefore, we compile a focused dataset of 265 compounds from data curated by CHEMBL [61]. The dataset includes different scaffolds including aminostyrylbenzofurans [62], 9-N-substituted ber-

berines [63], bisphenol A derivatives [64], caffeoylquinic acids [65], curcumins [66], flavonoids [67], tacrine-flavonoids hybrids [68], N-Arylnaphthylamines [69], indanes and indols [70, 71], N-phenylanthranilic acid analogs [72], piperidines [73] and quinone derivatives [74]. All the activity data were collected from a single assay type, namely the "Inhibition of $A\beta_{1\text{-}42}$ (or in some cases Aβ1-40) aggregation by thioflavin T assay". The activities are available as IC50 values. For this study, the cutoff was set to 5000 nm (i.e. compounds showing IC50 > 5000 nM were considered as inactive) in order to balance both active and inactive populations.

Virtual Screening

The fibril model ($A\beta_{1\text{-}42}$ pentamer) was first prepared by adding Gasteiger-Marsili [75] charges and then merging the non-polar hydrogens onto their respective heavy atoms using AutoDockTools [76]. Affinity potentials were pre-calculated by AutoGrid [76] for three atom types: C, HD (Hydrogen bond Donor) and OA (Oxygen hydrogen bond Acceptor), using a space grid of 1 Å. These grid maps were then applied to explore the pentamer surface with Autoligand [51] in order to search for putative binding sites.

Ligand preparation for docking was performed with OpenBabel [77]. The docking studies were all performed using AutoDock Vina 1.1.2 [48].

ROC curves for evaluating the performance of the fibril models were constructed using the ROCR package [78] from R software [79].

QM/MM Setup

The most important question when using the ONIOM scheme is the partitioning of the system into high and low level layers. In this work, we identified the binding site residues of the pentamer by using the free energy decomposition approaches (MM/GBSA). The side chains of the binding site residues that contribute with a $|\Delta G|$ higher than 1.0 $kcal.mol^{-1}$ in the per residue energy decomposition for both compounds **1** and **2** were included at the high-level QM layer, whereas the remainder of the complex system was included in the low-level MM layer. Only the geometry of the QM layer was fully optimized. Computations were carried out at ONIOM (B3LYP-D/6-31G(d):Amber) level. [80-83].

The MM parameters absent in the standard AMBER force field were included by using the generalized amber force field (GAFF) [84].

QTAIM (Atoms in Molecules Theory)

After the QM/MM calculation, the optimized geometries were used as input for the analysis by using the quantum theory atoms in molecules (QTAIM) [85] which was performed with the help of Multiwfn software [86], using the wave functions generated at the B3LYP-D/6-31G(d) level. This type of calculations have been used in recent works because they ensure a reasonable compromise between the wave function quality required to obtain reliable values of $\rho(r)$ and the available computer power, considering the extension of the system in study [8, 10].

CONCLUSIONS

When studying the effect of potential new antiaggregant agents, the ideal situation would be to perform these simulations in a large number of different forms of soluble oligomers. However, it is clear that this condition implies a very large task which is almost impossible to achieve, at least for systematic and routine studies. In this situation, particular models of soluble oligomer with the best features have to be chosen to be used as a molecular target. The results we obtained for the Aβ pentameric model after 2 μs of MD simulations have shown that this system is highly structured and stable. This study allowed us to distinguish characteristic features in different regions of the pentamer. The formation of cavities between adjacent chains in the region β1 allows the binding of compounds with potential beta sheet breaker activity whereas the opening of the TOP region might produce a channel for the insertion of hydrophobic compounds in the core and subsequent interactions with key residues involved in the oligomerization of Aβ fibrils. These structural features are important to take into account in order to use this model as a molecular target. This represents a clear advantage compared to the monomer or dimer models which are highly flexible structures with large numbers of possible conformers.

Here, we reported a virtual screening study indicating that the Aβ pentameric model is a reliable molecular target for this type of study; such conclusions are based on the ROC curves obtained, which indicate an acceptable degree of prediction for this model.

In addition, in a recent work we designed new mimetic peptides with antiaggregant properties by using a molecular modeling study using a pentameric model as a molecular target. To complete that study, we reported here a detailed analysis of the molecular interactions that take place between two active compounds and the Aβ pentameric model, which perturb the stability of the WT structure. This QTAIM study allows us to obtain information at sub-molecular level which is crucial to understand in detail the behavior of different potential antiaggregant agents. Once again the pentameric model used appears to be a good molecular target for this kind of study of molecular modeling.

Certainly, there are different structures which are candidates to be proposed as potential molecular targets for the design of new antiaggregant agents. Some might have certain advantages and also disadvantages with respect to the pentameric model proposed here. What is clear is that our results, as well as previously reported papers [45-47], contribute to establish the pentameric model as a potential molecular target for the design of new antiaggregant compounds. Also it should be noted that similar pentameric models have been successfully used by other authors [87, 88]. Even though this structure has been useful in our molecular modeling studies, it is necessary to perform further studies to ensure that this model is out of discussion and might be used as a molecular target for other analysis beyond the studies that we have reported here.

LIST OF ABBREVIATIONS

Aβ = Amyloid Beta

AD	=	Alzheimer's Disease
AL	=	AutoLigand
AUC	=	Area Under the Curve
BACE1	=	Beta Secretase 1
DR	=	Disordered Region
EPV	=	Energy Per Volume
GAFF	=	Generalized Amber Force Field
HD	=	Hydrogen bond Donor
MD	=	Molecular Dynamics
MM/GBSA	=	Molecular Mechanics/Generalized Born Surface Area
NMR	=	Nuclear Magnetic Resonance
OA	=	Oxygen hydrogen bond Acceptor
PDB	=	Protein Data Bank
QM	=	Quantum Mechanics
QTAIM	=	Quantum Theory of Atoms in Molecules
ROC	=	Receiver Operating Characteristic curves
Se	=	Sensitivity
1-Sp	=	1-Specificity
TEM	=	Transmission Electron Microscopy
ThT	=	Thioflavin T
WT	=	Wild type

CONFLICT OF INTEREST

The authors confirm that this article content has no conflicts of interest.

ACKNOWLEDGEMENTS

Grants from Universidad Nacional de San Luis (UNSL) partially supported this work. E.E.B.G. thanks CONICET-Argentina for a doctoral fellowship. R.D.E. and S.A.A. are staff members of the National Research Council of Argentina (CONICET-Argentina).

SUPPLEMENTARY MATERIALS

Supplementary material is available on the publisher's web site along with the published article.

REFERENCES

[1] Fandrich, M. On the structural definition of amyloid fibrils and other polypeptide aggregates. *Cell. Mol. Life. Sci.,* **2007**, *64*, 2066-2078.

[2] Walker, L.C.; LeVine, H. The cerebral proteopathies: neurodegenerative disorders of protein conformation and assembly. *Mol. Neurobiol.,* **2000**, *21*, 83-95.

[3] Hardy, J. Expression of normal sequence pathogenic proteins for neurodegenerative disease contributes to disease risk: "permissive templating" as a general mechanism underlying neurodegeneration. *Biochem. Soc. Trans.*, **2005**, *33*, 578-581.

[4] Ferri, C.P.; Prince, M.; Brayne, C.; Brodaty, H.; Fratiglioni, L.; Ganguli, M.; Hall, K.; Hasegawa, K.; Hendrie, H.; Huang, Y.; Jorm, A.; Mathers, C.; Menezes, P.R.; Rimmer, E.; Scazufca, M. Global prevalence of dementia: a Delphi consensus study. *Lancet*, **2005**, *366*, 2112-2117.

[5] Arkin, M.R.; Wells, J.A. Small-molecule inhibitors of protein–protein interactions: progressing towards the dream. *Nat. Rev. Drug. Disc.,* **2004**, *3*, 301-317.

[6] Whittle, P.J.; Blundell, T. L. Protein structure--based drug design *Annu. Rev. Biophys. Biomol. Struct.* **1994**, *23*, 349-375.

[7] Párraga, J.; Cabedo, N.; Andujar, S.; Piqueras, L.; Moreno, L.; Galán, A.; Angelina, E.; Enriz, R.D.; Ivorra, M.D.; Sanz, M.J.; Cortes, D. 2,3,9- and 2,3,11-trisubstituted tetrahydroproto berberines as D2 dopaminergic ligands. *Eur. J. Med. Chem.* **2013**, *68*, 150-166.

[8] Tosso, R.D.; Andujar, S.A.; Gutierrez, L.; Angelina, E.; Rodríguez, R.; Nogueras, M.; Baldoni, H.; Suvire, F. D.; Cobo, J.; Enriz, R. D. Molecular modeling study of dihydrofolate reductase inhibitors. Molecular dynamics simulations, quantum mechanical calculations, and experimental corroboration. *J. Chem. Inf. Model.*, **2013**, *53*, 2018-2032.

[9] Andujar, S.; Suvire, F.; Berenguer, I.; Cabedo, N.; Marin, P.; Moreno, L.; Dolores Ivorra, M.; Cortes, D.; Enriz, R.D. Tetrahydroisoquinolines acting as dopaminergic ligands. A molecular modeling study using MD simulations and QM calculations. *J. Mol. Model*, **2012**, *18*, 419-431.

[10] Andujar, S.A.; Tosso, R.D.; Suvire, F.D.; Angelina, E.; Peruchena, N.; Cabedo, N.; Cortes, D.; Enriz, R.D. Searching the "biologically relevant" conformation of dopamine: a computational approach. *J. Chem. Inf. Model.*, **2012**, *52*, 99−112.

[11] Citron, M. Alzheimer's disease: strategies for disease modification. *Nat. Rev. Drug. Discov.*, **2010**, *9*, 387-398.

[12] Mc Donald, R.J.; Craig, L.; Hong, N. The etiology of age-related dementia is more complicated than we think. *Behav. Brain Res.,* **2010**, *214*, 3-11.

[13] Benilova, I.; Karran, E.; De Strooper, B. The toxic Aβ oligomer and Alzheimer's disease: an emperor in need of clothes. *Nat Neurosci.*, **2012**, *15*, 349-357.

[14] Armstrong, R.A. The pathogenesis of Alzheimer's disease: a re-evaluation of the "Amyloid Cascade Hypothesis." *Int. J. Alzheimers Dis.*, **2011**, 2011:630865.

[15] Gutierrez, L.J.; Enriz, R.D.; Baldoni, H.A. Structural and thermodynamic characteristics of the exosite binding pocket on the human BACE1: a molecular modeling approach. *J. Phys. Chem. A*, **2010**, *114*, 10261-10269.

[16] Atwal, J.K.; Chen, Y.; Chiu, C.; Mortensen, D.L.; Meilandt, W.J.; Liu, Y.; Heise, C.E.; Hoyte, K.; Luk, W.; Lu, Y.; Peng, K.; Wu. P.; Rouge, L.; Zhang, Y.; Lazarus, R.A.; Scearce-Levie,. K.; Wang, W.; Wu, Y.; Tessier-Lavigne, M.; Watts, R.J. A therapeutic antibody targeting BACE1 inhibits amyloid-β production *in vivo*. *Sci. Transl. Med*, **2011**, *3*, 84-84.

[17] Zhou, L.; Chávez-Gutiérrez, L.; Bockstael, K.; Sannerud, R.; Annaert, W.; May, P.C.; Karran, E.; De Strooper, B. Inhibition of beta-secretase *in vivo* via antibody binding to unique loops (D and F) of BACE1. *J. Biol. Chem.*, **2011**, *286*, 8677-8687.

[18] Ghosh, A.K.; Shin, D.W.; Downs, D.; Koelsch, G.; Lin, X.L.; Ermolieff, J.; Tang, J. Design of potent inhibitors for human brain memapsin 2 (β-Secretase), *J. Am. Chem. Soc*., **2000**, *122*, 3522-3523.

[19] Tang, J.; Hong, L.; Ghosh, A. K. *Aspartic Acid Proteases as Therapeutic Targets*. Wiley-VCH, **2010**, 45, 413-440.

[20] Roberts, B.E.; Shorter, J. Escaping amyloid fate. *Nat. Struct. Mol. Biol.*, **2008**, *15*, 544-546.

[21] Wang, W. Protein aggregation and its inhibition in biopharmaceutics. *Int. J. Pharm.*, **2005**, *289*, 1-30.

[22] Bartolini, M.; Andrisano, V. Strategies for the inhibition of protein aggregation in human diseases. *ChemBioChem.*, **2010**, *11*, 1018-1035.

[23] Esteras-Chopo, A.; Pastor, M.T.; Serrano, L.; Lopez de la Paz, M. New strategy for the generation of specific D-peptide amyloid inhibitors. *J. Mol. Biol.*, **2008**, *377*, 1372-1381.

[24] Fradinger, E.A.; Monien, B.H.; Urbanc, B.; Lomakin, A.; Tan, M.; Li, H.; Spring, S.M.; Condron, M.M.; Cruz, L.; Xie, C.W.; Benedek, G.B.; Bitan, G. C-terminal peptides coassemble into Aβ42 oligomers and project neurons against Aβ42-induced neurotoxicity. *Proc. Natl. Acad. Sci. USA*, **2008**, *105*, 14175-14180.

[25] Doig, A.J. Peptide inhibitors of β-amyloid aggregation. *Curr. Opin. Drug Discov. Devel.*, **2007**, *10*, 533-539.

[26] Cheng, P.N.; Liu, C.; Zhao, M.; Eisenberg; D.; Nowick, J.S. Amyloid β-sheet mimics that antagonize protein aggregation and reduce amyloid toxicity. *Nat. Chem.*, **2012**, *4*, 927-933.

[27] van Groen, T.; Wiesehan, K.; Funke, S.A.; Kadish; I.; Nagel-Steger, L.; Willbold, D. Reduction of Alzheimer's disease amyloid plaque load in transgenic mice by D3, A D-enantiomeric peptide identified by mirror image phage display. *Chem. Med. Chem.*, **2008**, *3*, 1848-1852.

[28] Belluti, F.; Rampa, A.; Gobbi, S.; Bisi, A. Small-molecule inhibitors/modulators of amyloid-β peptide aggregation and toxicity for the treatment of Alzheimer's disease-A patent review (2010–2012). *Expert. Opin. Ther. Pat.*, **2013**, *23*, 581-596.

[29] Re, F.; Airoldi, C., Zona, C.; Masserini, M.; La Ferla, B.; Quattrocchi, N. β amyloid aggregation inhibitors: small molecules as candidate drugs for therapy of Alzheimer's disease. *Curr. Med. Chem.*, **2010**, *17*, 2990-3006.

[30] Bertoncini, C.W.; Jung, Y.S.; Fernandez, C.O.; Hoyer, W.; Griesinger, C.; Jovin, T.M.; Zweckstetter, M. Release of long-range tertiary interactions potentiates aggregation of natively unstructured α-synuclein. *Proc. Natl. Acad. Sci. U.S.A.*, **2005,** *102*, 1430-1435.

[31] Dedmon, M.M.; Lindorff-Larsen, K.; Christodoulou, J.; Vendruscolo, M.; Dobson, C.M. Mapping long-range interactions in r-synuclein using spin-label NMR and ensemble molecular dynamics simulations. *J. Am. Chem. Soc.*, **2005**, *127*, 476-477.

[32] Mukrasch, M.D.; Markwick, P.; Biernat, J.; von Bergen, M.; Bernado, P.; Griesinger, C.; Mandelkow, E.; Zweckstetter, M.; Blackledge, M. Highly populated turn conformations in natively unfolded tau protein identified from residual dipolar couplings and molecular simulation. *J. Am. Chem. Soc.*, **2007**, *129*, 5235-5343.

[33] Teplow, D.B.; Lazo, N.D.; Bitan, G.; Bernstein, S.; Wyttenbach, T.; Bowers, M.T.; Baumketner, A.; Shea, J.E.; Urbanc, B.; Cruz, L.; Borreguero, J.; Stanley, H.E. Elucidating amyloid beta-protein folding and assembly: a multidisciplinary approach. *Acc. Chem. Res.,* **2006**, *39*, 635-–645.

[34] Soto, C.; Estrada, L. D.; Protein misfolding and neurodegeneration. *Arch. Neurol*., **2008**, *65*, 184-189.

[35] Zhu, M.; De Simone, A.; Schenk, D.; Toth, G.; Dobson, C.M.; Vendruscolo, M. Identification of small-molecule binding pockets in the soluble monomeric form of the Ab42 peptide. *J. Chem. Phys.*, **2013** ,*139*, 035101.

[36] Lemkul, J.; Bevan, D.R. Morin inhibits the early stages of amyloid β-peptide aggregation by altering tertiary and quaternary interactions to produce "off- pathway" structures. *Biochemistry*, **2012**, *30*, 5990-6009.

[37] Hou, L.M.; Shao, H.Y.; Zhang, Y.B.; Li, H.; Menon, N.K.; Neuhaus, E.B.; Brewer, J.M.; Byeon, I.J.L.; Ray, D.G.; Vitek, M.P.; Iwashita, T. R.; Makula, A.; Przybyla, A.B.; Zagorski, M.G. Solution NMR studies of the A-beta(1-40) and A-beta(1-42) peptides establish that the Met35 oxidation state affects the mechanism of amyloid formation. *J. Am. Chem. Soc.*, **2004**, *126*, 1992-2005.

[38] Zhang, S.; Iwata, K.; Lachenmann, M.J.; Peng, J.W.; Li, S.; Stimson, E.R.; Lu, Y.; Felix, A.M.; Maggio, J.E.; Lee, J.P. The Alzheimer's peptide a beta adopts a collapsed coil structure in water. *J. Struct. Biol*., **2000**, *130*, 130-141.

[39] Kassler, K.; Horn, A.H.C.; Sticht, H. Effect of pathogenic mutations on the structure and dynamics of Alzheimer's A-beta 42-amyloid oligomers. *J. Mol. Model.*, **2010**, *16*, 1011–1020.

[40] Kittner, M.; Knecht, V.J. Disordered versus fibril-like amyloid beta (25-35) dimers in water: structure and thermodynamics. *J. Phys. Chem. B*, **2010**, *114*, 15288–15295.

[41] Cô té S.; Laghaei R.; Derreumaux P.; Mousseau N. Distinct dimerization for various alloforms of the amyloid-beta protein: Aβ1−40,Aβ1−42, and Aβ1−40(D23N). *J. Phys. Chem. B.*, **2012**, *116*, 4043-4055.

[42] Nguyen P.; Derreumaux P. Understanding amyloid fibril nucleation and Aβ oligomer/drug interactions from computer simulations. *Acc. Chem. Res.*, **2014**, *47*, 603-611.

[43] Makin, O.S.; Serpell, L.C. Structures for amyloid fibrils. *FEBS J.,* **2005**, *272*, 5950-5961.

[44] Tycko, R. Solid-state NMR studies of amyloid fibril structure. *Annu. Rev. Phys. Chem.*, **2011**, *62*, 279-299.

[45] Masman, M.F.; Eisel, U.L.M.; Csizmadia, I.G.; Penke, B.; Enriz, R.D.; Marrink, S.J.; Luiten, P.G.M. In silico study of full-length amyloid β 1-42 tri- and penta-oligomers in solution. *J. Phys. Chem. B.,* **2009**, *113*, 11710-11719.

[46] Barrera Guisasola, E.E.; Andujar, S.A.; Hubin, E.; Broersen, K.; Méndez, L.; Delpiccolo, C.M.L; Masman, M.F.; Rodríguez, A.M.; Enriz, R.D. New mimetic peptides inhibitors of Aβ aggregation. Molecular guidance for rational drug design. *Eur. J. Med. Chem.,* **2015** (submitted for publication).

[47] Andujar, S.A.; Lugli, F.; Höfinger, S.; Enriz, R.D.; Zerbetto, F. Amyloid-b fibril disruption by C60—molecular guidance for rational drug design. *Phys. Chem. Chem. Phys.*, **2012**, *14*, 8599-8607.

[48] Trott, O.; Olson, A.J. AutoDock Vina: Improving the speed and accuracy of docking with a new scoring function, efficient optimization, and multithreading. *J. Comput. Chem.*, **2010**, *31*, 455-461.

[49] Lührs, T.; Ritter, C.; Adrian, M.; Riek-Loher, D.; Bohrmann, B.; Döbeli, H. 3D structure of Alzheimer's amyloid-beta(1-42) fibrils. *Proc. Natl. Acad. Sci. USA.*, **2005**, *102*, 17342-17347.

[50] Zhao, J.H.; Liu, H.L.; Elumalai, P.; Chen, W.H.; Men L.C.; Liu, K.T. Molecular modeling to investigate the binding of congo red toward GNNQQNY protofibril and in silico virtual screening for the identification of new aggregation inhibitors. *J. Mol. Model.*, **2013**, *19*, 151-62.

[51] Harris, R.; Olson, A.J.; Goodsell, D.S. Automated prediction of ligand-binding sites in proteins. *Proteins,* **2008**, *70*, 1506-1517.

[52] Hoffmann, R.D. Pharmacophores and pharmacophore searches, Wiley-VCH, **2006**, Vol. 32.

[53] Elser, W.P.; Stimson, E.R.; Ghilardi, J.R.; Vinters, H.V.; Lee, J.P.; Mantyh, P.W.; Maggio J.E. *In vitro* growth of Alzheimer's disease β-amyloid plaques displays first-order kinetics. *Biochemistry*, **1996**, *35*, 749-757.

[54] Hilbich, C.; Kisters-Woike, B.; Reed, J.; Masters C.L.; Beyreuther, K. Substitutions of hydrophobic amino acids reduce the amyloidogenicity of Alzheimer's disease beta A4 peptides. *J. Mol. Biol.*, **1992**, *20*, 460-473.

[55] Jorgensen, W.L.; Chandrasekhar, J.; Madura, J.D.; Impey, R.W.; Klein, M.L. Comparison of simple potential functions for simulating liquid water. *J. Chem. Phys.*, **1983**, 79, 926-935.

[56] Case, D.A.; Cheatham, T.E.; Darden, T.; Gohlke, H.; Luo, R.; Merz Jr., K.M.; Onufriev, A.; Simmerling, C.; Wang B.; Woods, R.J. The Amber biomolecular simulation programs. *J. Comput. Chem.*, **2005**, *26*, 1668-1688.

[57] Darden, T.; York, D.; Pedersen, L. Particle mesh Ewald: An *N*-log(*N*) method for Ewald sums in large systems *J. Chem. Phys.*, **1993**, *98*, 10089-10092.

[58] Essmann, U.; Perera, L.; Berkowitz, M.L.; Darden, T.; Lee, H.; Pedersen, L.G. A smooth particle mesh Ewald method. *J. Chem. Phys.*, **1995**, *103*, 8577-8593.

[59] Ryckaert, J.; Ciccotti, G.; Berendsen, H.J. Numerical integration of the cartesian equations of motion of a system with constraints: molecular dynamics of n-alkanes. *J. Comput. Phys.*, **1977**, *23*, 327-341.

[60] Wiggers, H.J.; Rocha, J.R.; Cheleski, J.; Montanari C. Integration of ligand- and target-based virtual screening for the discovery of cruzain inhibitors. *Mol. Inform.*, **2011,** *30* ,565-578.

[61] Gaulton, A.; Bellis, L.J.; Bento, A.P.; Chambers J.; Davies, M.; Hersey, A. ChEMBL: a large-scale bioactivity database for drug discovery. *Nucleic Acids. Res.*, **2012,** D1100–D1107.

[62] Byun, J.H.; Kim, H.; Kim, Y.; Mook-Jung, I.; Kim, D.J.; Lee, W.K,.; Yoo, K.H. Aminostyrylbenzofuran derivatives as potent inhibitors for Abeta fibril formation. *Bioorg. Med. Chem. Lett.,* **2008***, 18***,** 5591-5593.

[63] Shan, W.-J.; Huang, L.; Zhou, Q.; Meng, F.-C.; Li, X.-S. Synthesis, biological evaluation of 9-N-substituted berberine derivatives as multi-functional agents of antioxidant, inhibitors of acetyl cholinesterase, butyrylcholinesterase and amyloid-β aggregation. E*ur. J. Med. Chem.,* **2011***, 46***,** 5885-5893.

[64] Zhou, Y.; Jiang, C.; Zhang, Y.; Liang, Z; Liu, W.; Wang, L.; Luo, C,; Zhong, T.; Sun, Y.; Zhao, L.; Xie, X.; Jiang, H.; Zhou, N.; Liu D.; Liu, H.; Structural optimization and biological evaluation of substituted bisphenol A derivatives as beta-amyloid peptide aggregation inhibitors. *J. Med. Chem.,* **2010,** *53***,** 5449-5466.

[65] Miyamae, Y.; Kurisu, M.; Murakami, K.; Han, J.; Isoda, H.; Irie, K.; Shigemori, H.; Protective effects of caffeoylquinic acids on the aggregation and neurotoxicity of the 42-residue amyloid β-protein. *Bioorg. Med. Chem.,* **2012**, *20***,** 5844-5849.

[66] Chen, S.Y.; Chen, Y.; Li, Y.P.; Chen, S.H.;Tan, J.H.; Ou T.M.; Gu, L.Q.; Huang, Z.S. Design, synthesis, and biological evaluation of curcumin analogues as multifunctional agents for the treatment of Alzheimer's disease. *Bioorg. Med. Chem.,* **2011**, *19***,** 5596-5604.

[67] Carver, J.; Duggan, P.J.; Ecroyd, H.;Liu, Y.; Meyer, A.G.; Tranberg, C.E. Carboxymethylated-kappa-casein: a convenient tool for the identification of polyphenolic inhibitors of amyloid fibril formation. *Bioorg. Med. Chem.,* **2010**, *18*, 222-228.

[68] Li, S.Y.; Wang, X.B.; Xie, S.S.; Jiang, N.; Wang, K.D.; Yao, H.Q.; Sun, H.B., Kong, L.Y. Multifunctional tacrine-flavonoid hybrids with cholinergic, β-amyloid-reducing, and metal chelating properties for the treatment of Alzheimer's disease. *Eur. J. Med. Chem.,* **2013**, *69*, 632-646.

[69] Di Santo, R.; Costi, R.; Cuzzucoli, G.; Pescatori, L.; Rosi, F.; Scipione, L.; Celona, D.; Vertechy, M.; Ghirardi, O.; Piovesan, P.; Marzi, M.; Caccia, S.; Guiso, G.; Giorgi, F.; Minetti, P. Design, synthesis, and structure-activity relationship of N- aryl naphthylamine derivatives as amyloid aggregation inhibitors. *J. Med. Chem.*, **2012**, *55*, 8538-8548.

[70] Catto, M.; Aliano, R.; Carotti, A.; Cellamare, S.; Palluotto, F.; Purgatorio, R.; De Stradis, A. Campagna F. Design, synthesis and biological evaluation of indane-2-arylhydrazinylmethylene-1,3-diones and indol-2-aryldiazenylmethylene-3-ones as beta-amyloid aggregation inhibitors. *Eur. J. Med. Chem.,* **2010**, *45*, 1359-1366.

[71] Campagna, F.; Catto, M.; Purgatorio, R.; Altomare, C.D.; Carotti, A.; De Stradis, A.; Palazzo, G. Synthesis and biophysical evaluation of arylhydrazono-1H-2-indolinones as β-amyloid aggregation inhibitors. *Eur. J. Med. Chem.,* **2011**, *46*, 275-284.

[72] Simons, L.J.; Caprathea, B.W.; Callahana, M.; Grahama, J.M.; Kimurab, T.; Laia, Y.; LeVine, H.; Lipinskia, W.; Sakkaba, A.T.; Tasakib, Y.; Walkera, L.C.; Yasunagab, T.; Yea, Y.; Zhuanga, N.; Augelli-Szafrana, C.E. The synthesis and structure-activity relationship of substituted N-phenyl anthranilic acid analogs as amyloid aggregation inhibitors. *Bioorg. Med. Chem. Lett.,* **2009***, 19***,** 654-657.

[73] Kwon, Y.E.; Park, J.Y.; No, K.T.; Shin, J.H.; Lee, S.K.; Eun, J.S.; Yang, J.H.; Shin, T.Y.; Kim, D.K.; Chae, B.S.; Leem, J.Y.; Kim, KH. Synthesis, *in vitro* assay, and molecular modeling of new piperidine derivatives having dual inhibitory potency against acetylcholinesterase and Abeta1-42 aggregation for Alzheimer's disease therapeutics. *Bioorg. Med. Chem.*, **2007**, *15***,** 6596-6607.

[74] Prati, F.; Bartolini, M.; Simoni, E.; De Simone, A.; Pinto, A.; Andrisano, V.; Bolognesi, M.L. Quinones bearing non-steroidal anti-inflammatory fragments as multitarget ligands for Alzheimer's disease. *Bioorg. Med. Chem. Lett.*, **2013**, *23*, 6254-6258.

[75] Gasteiger, J.; Marsili, M.; Iterative partial equalization of orbital electronegativity-a rapid access to atomic charges. *Tetrahedron*, **1980**, *36*, 3219-3228.

[76] Morris, G.M.; Huey, R.; Lindstrom, W.; Sanner, M.F.; Belew, R.K.; Goodsell, D.S.; Olson, A.J. Autodock4 and AutoDockTools4: automated docking with selective receptor flexiblity. *J. Comput. Chem.,* **2009**, *16*, 2785-91.

[77] O'Boyle, N.M.; Banck, M.; James, C.A.; Morley, C.; Vandermeersch, T.; Hutchison, G.R. Open Babel: An open chemical toolbox. *J. Cheminf.,* **2011**, *3*, 33.

[78] Sing, T.; Sander, O.; Beerenwinkel, N.; Lengauer, T. ROCR: visualizing classifier performance in R. *Bioinformatics,* **2005**, *21*, 3940-3941.

[79] R Core Team (2013). R: A language and environment for statistical computing. R Foundation for Statistical Computing, Vienna, Austria. URL http://www.R-project.org/

[80] Becke, AD. Density-functional exchange-energy approximation with correct asymptotic behavior. *Phys. Rev. A.*, **1988**, *38*, 3098-3100.

[81] Lee, C.; Yang, W.; Parr, R.G.; Development of the Colle-Salvetti correlation-energy formula into a functional of the electron density. *Phys. Rev. B*, **1988**, *37*, 785-789.

[82] Grimme, S.; Semiempirical GGA-type density functional constructed with a long-range dispersion correction. *J. Comp. Chem.,* **2006**, *27*, 1787-1799.

[83] Cornell, W.D.; Cieplak, P.; Bayly, C.I.; Gould, I.R.; Merz, K.M.; Ferguson, D.M.; Spellmeyer, D.C.; Fox, T.; Caldwell, J.W.; Kollman, P.A. A second generation force field for the simulation of proteins, nucleic acids, and organic molecules. *J. Am. Chem. Soc.,* **1995**, *117*, 5179-5197.

[84] Wang, J.; Wolf, R.M.; Caldwell, J.W.; Kollman, P.A.; Case, D.A. Development and testing of a general amber force field. *J. Comput. Chem.,* **2004**, *25*, 1157-1174.

[85] Bader, R.F.W. Atoms in molecules. *Acc. Chem. Res.,* **1985**, *18*, 9-15.

[86] Lu, T.; Chen, F. Multiwfn: a multifunctional wave-function analyzer. *J. Comput. Chem.*, **2012**, *33*, 580-592.

[87] Lemkul, J.; Bevan, D.R. Assessing the stability of Alzheimer's amyloid protofibrils using molecular dynamics. *J. Phys. Chem. B*, **2010**, *114*, 1652-1660.

[88] Lemkul, J.; Bevan, D.R. Destabilizing Alzheimer's Aβ42 protofibrils with morin: mechanistic insights from molecular dynamics simulations. *Biochemistry*, **2010**, *49*, 3935-3946.

Received: ????????????????? Revised: ????????????????? Accepted: ?????????????????